Ab Intio Based Potential Energy Surfaces and Franck−Condon Analysis of Ionization Thresholds of Cyclic-C_3H and Linear-C_3H†

Yimin Wang,‡ Bastiaan J. Braams,§ and Joel M. Bowman*,‡

Department of Chemistry and Cherry L. Emerson Center for Scientific Computation and Department of Mathematics and Computer Science, Emory University, Atlanta, Georgia 30322

Received: November 18, 2006; In Final Form: December 20, 2006

We report a Franck−Condon analysis in reduced dimensionality of the ionization thresholds of linear(*l*)-C_3H and cyclic(*c*)-C_3H using MP2-based potential energy surfaces and CCSD(T)/aug-cc-pVTZ calculations of electronic energies at selected geometries. The potential energy surfaces are fits to tens of thousands of MP2/aug-cc-pVTZ energies for the neutral and cation systems. These fits properly describe the invariance of the potential with respect to all permutations of the three C atoms. The realism of the potential surfaces is assessed by comparing stationary-point structures, energies, and normal-mode frequencies with previous high-level ab initio calculations. Several key vibrational modes in this ionization process are located at saddle points and so a numerical approach to obtain the Franck−Condon factors for those modes is done. On the basis of this analysis combined with a simple harmonic treatment of the energies of the remaining modes and key electronic energy differences obtained with CCSD(T)/aug-cc-pVTZ calculations, we find the threshold ionization energy of *l*-C_3H to be 9.06 eV and for *c*-C_3H we estimate the threshold to be in the range 9.70−9.76 eV. We estimate these values are accurate to within ±0.05 eV.

I. Introduction

The reaction of C(^{3}P) with C_2H_2 to form C_3+ H_2 and C_3H + H has attracted a considerable amount of attention, both experimentally[1−15] and theoretically,[16−22] due in part to the importance of the reaction in the interstellar medium, where the C_3H product has been detected. The experiment is challenging if ones wants to distinguish between the two nearly isoenergetic isomers of C_3H, i.e., linear and cyclic C_3H, denoted *l*-C_3H and *c*-C_3H, respectively, because conventional mass-spectrometric detection cannot be used for this purpose.

One technique that can be used to distinguish isomers formed in chemical reactions is threshold photoionization spectroscopy;[23] this could be a fruitful approach for the identification of the *l*-C_3H and *c*-C_3H products of the C(^{3}P) with C_2H_2 reaction. Previous studies have been reported on aspects of the ionization of C_3H. Ikuta reported the ionization energy of *c*-C_3H to be 9.06 eV at the MRCI/aug-cc-pVTZ level of theory/basis.[24] Chaudhuri et al.[25] performed high-level ab initio calculations of energy differences between *l*-C_3H and *c*-C_3H and the respective cations, and vertical ionization energies. They reported vertical ionization energies of 9.21 eV for *l*-C_3H using their calculated geometry and 9.33 eV using the experimental geometry, and 10.66 eV for *c*-C_3H for both their calculated and experimental geometry. Clearly there are significant differences between these two sets of calculations for the ionization of *c*-C_3H. Also, it should be noted that these calculations did not consider zero-point energy corrections and did not report Franck Condon factors for the ionization.

These systems are interesting and challenging for several reasons. Perhaps the most interesting one is, as tentatively reported earlier[24] and verified here, *c*-C_3H^+ does not exist as a stable minimum, but as a first-order saddle point. Thus the standard model of vertical photoionization of *c*-C_3H, which is a stable minimum, is problematic. A second complication is that the *l*-C_3H minimum has been reported to be linear or slightly bent, depending on the level of ab initio theory and basis, whereas the *l*-C_3H^+ minimum is linear.

We investigate these interesting aspects of the photoionization of both isomers of C_3H in this paper. We do this by constructing full-dimensional potential energy surfaces for the neutral and cationic C_3H systems based on MP2/aug-cc-pVTZ calculations, doing reduced dimensionality calculations of Franck−Condon factors using these surfaces, and finally using CCSD(T)/aug-cc-pVTZ energies for certain key electronic energy differences.

The calculations and some details of the potential energy surface (PES) fitting are given in the next section as are relevant properties of the PESs and comparisons with previous ab initio calculations at stationary points. The reduced dimensionality Franck−Condon calculations are described and presented in section III and a summary and conclusions are given in section IV.

II. Ab Initio Calculations and the Potential Energy Surfaces

We performed tens of thousands of MP2/aug-cc-pVTZ calculations for C_3H and C_3H^+ using MOLPRO 2002[26] to determine the energies for use in creating full-dimensional PESs. For both surfaces we used a many-body expansion with polynomials that are invariant with respect to permutation of the three C atoms up to total degree 8 for all the terms. This fitting approach used has been applied and described in detailed elsewhere[27,28] and so we are brief here with the description. The one-body potentials are fixed, and then we have a total of 744 free coefficients for the two-body, three-body, and four-body terms, altogether.

† Part of the special issue "James A. Miller Festschrift".

* Corresponding author. E-mail: jmbowma@emory.edu.

‡ Department of Chemistry and Cherry L. Emerson Center for Scientific Computation.

§ Department of Mathematics and Computer Science.

10.1021/jp0676787 CCC: $37.00
Published on Web 01/25/2007

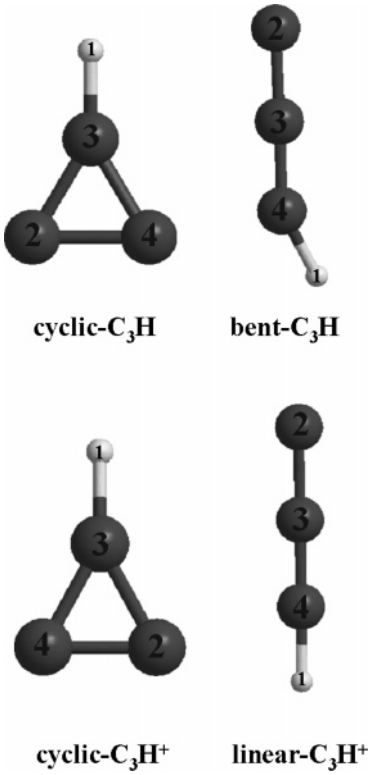

Figure 1. Equilibrium minimum structures of *l*-C_3H, *l*-C_3H^+, *c*-C_3H, and the saddle point structure of *c*-C_3H^+.

We used 42 186 configurations for the case of C_3H and 17 812 for the case of C_3H^+. The present fits are semiglobal in that they do not describe fragmentation; however, they do describe the isomerization of C_3H and C_3H^+. An assessment of the realism of these PESs will be given next, where geometries, energies and normal-mode frequencies at stationary points will be presented and compared with previous ab initio calculations, generally obtained with higher levels of theory.

Stationary points were located on these PESs. These are shown graphically in Figure 1, where as seen the PES finds the minimum of *l*-C_3H to be slightly bent. Comparison of the structures and energies with previous benchmark ab initio calculations[24,15] are given Table 1. There is generally excellent agreement for all structures with previous high-level calculations, with the only slightly problematic one being the minimum for *l*-C_3H. As seen, two sets of previous CCSD(T) calculations, done with somewhat different basis sets,[15] give slightly different structures for the minimum, one is slightly bent and the other is linear, depending on the basis. An extensive study of this issue was done by Ochsenfeld et al.[15] At the CCSD(T)/cc-pVQZ level of theory and basis set they found that the linear structure is slightly lower (by 66 cm^{-1}) than the bent structure, using geometries optimized with CCSD(T)/TZP calculations. Those latter calculations are the ones cited in this table. Clearly these calculations indicate either a double minimum potential with a small barrier in the bending coordinate or a flat, anharmonic potential with a linear minimum. The present PES indicates the former. We will show in the next section that the ground state vibrational wave function for this mode is highly delocalized over the two minima and saddle point and so the issue of whether the potential is a double well or a single well is not very significant.

Table 2 contains the normal-mode frequencies and harmonic zero-point energies obtained from the PESs and results from previous ab initio calculations.[15,29] It also contains a comparison of energies, relative to the global minimum energy of *c*-C_3H, of previous CCSD(T)/aug-cc-pVTZ calculations by Ikuta[24] at the geometries in Table 1 and also new CCSD(T)/aug-cc-pVTZ that we did at the PES stationary points. We see good agreement between the PES normal-mode frequencies for *l*-C_3H with those from previous CCSD(T)/TZP calculations,[15] with the exception of modes 4 and 6. For *c*-C_3H the comparison shows good agreement with the calculations of Stanton[29] except for mode 1. As he discussed, there is a strong pseudo Jahn−Teller interaction, which is not accounted for in the present MP2 calculations and so that could be affecting the frequency of mode 1 from the PES.

TABLE 1: Geometries of Stationary Structures for Both C_3H Radical and C_3H Cation (Lengths in Angstroms; Angles in Degrees)

	Cyclic-C_3H	
	PES	RCCSD(T)/aug-cc-pVTZ[a]
R(C3-H)	1.0790	1.0800
R(C2−C3)	1.3820	1.3809
R(C2−C4)	1.3847	1.3818
∠H-C3−C2	150.01	149.98

	Cyclic-C_3H^+	
	PES	RCCSD(T)/aug-cc-pVTZ[a]
R(C3-H)	1.0842	1.0883
R(C2−C3)	1.3799	1.3831
R(C2−C4)	1.2939	1.3076
∠H-C3−C2	152.03	151.79

	Linear-C_3H		
	PES	RCCSD(T)/aug-cc-pVTZ[a]	CCSD(T)/TZP[b]
R(C4-H)	1.068	1.0699	1.072
R(C2−C3)	1.315	1.3480	1.336
R(C3−C4)	1.266	1.2473	1.253
∠H-C4−C3	150.8	180	156.5
∠C2−C3-C4	179.4	180	174.0

	Linear-C_3H^+	
	PES	RCCSD(T)/aug-cc-pVTZ[a]
R(C4-H)	1.0820	1.0811
R(C2−C3)	1.3378	1.3482
R(C3−C4)	1.2539	1.2473
∠H-C4−C3	180.0	180.00

[a] Reference 24. [b] Reference 7.

TABLE 2: Harmonic Frequencies (cm^{-1}) and Zero-Point Energies (ZPE) from the Potential Energy Surfaces (PES) and Other Sources, As Indicated, as Well as Energies (cm^{-1}) Relative to the Global Minimum, *c*-C_3H, from the PESs, Previous Sources, and the Present CCSD(T)/aug-cc-pVTZ Calculations Done at the PES Geometries

	l-C_3H-linear	*l*-C_3H-bent	*l*-C_3H^+	*c*-C_3H	*c*-C_3H^+
mode 1	417i[a]		110[a]		
mode 2	417i	259,[a] 208[b]	110	*718*,[a] 281[c]	461i[a]
mode 3	289	289, 351	*808*	917, 898	873
mode 4	289	581, 369	*808*	939, 957	1053
mode 5	1162	1189, 1170	1199	1175, 1244	1457
mode 6	1928	2011, 1876	2164	1508, 1639	1808
mode 7	3387	3339, 3380	3291	3261, 3330	3241
ZPE	3527	3833, 3677	4245	4260, 4175	4216
PES	2736	2436	74296	0	79963
ab initio[d]	1014	1105	73197	0	79123
ab initio[e]	949		73095	0	79049

[a] Present PES. [b] CCSD(T)/TZP calculations from ref 15. [c] CCSD/EOM calculations from ref 29. [d] Present CCSD(T)/aug-cc-pVTZ calculations. [e] CCSD(T)/aug-cc-pVTZ calculations from ref 24.

Next consider a comparison of the energies given in the table. The PES results are in good agreement with the present and previous CCSD(T)/aug-cc-pVTZ[24] values, which are themselves in excellent agreement, considering the slight differences in the geometries used to obtain these energies. The PES energies and their difference for *l*-C_3H (linear and bent) are higher than the CCSD(T) ones and the order is reversed. This is essentially an error due to the MP2 method. For the present purpose of this paper the significant number is the height of the PES barrier between the linear and bent geometries of *l*-C_3H, which is 300 cm^{-1}. Although this value is higher than the 66 cm^{-1} barrier obtained at the highest level ab initio calculations, CCSD(T)/cc-pVQZ, obtained at the CCSD(T)/TZP geometries,[15] we will show in the next section that the PES almost certainly describes the zero-point wavefunction *l*-C_3H qualitatively correctly.

To conclude this section, we note that rough estimates of the ionization thresholds can be determined from the results in Table 2 using the present CCSD(T)/aug-cc-pVTZ calculations. For *c*-C_3H the "vertical" ionization energy to the *c*-C_3H^+ saddle point is 9.8 eV and the vertical ionization energy for *l*-C_3H (linear) to *l*-C_3H^+ is roughly 8.95 eV. Given that some of the stationary points used in these estimates are saddle points, we stress that these can only be regarded as rough estimates. A treatment of the vibrational wave functions for the highly anharmonic imaginary modes is needed for a more precise treatment of the ionization process. We address this in the next section where we present a reduced dimensionality Franck−Condon analysis for these highly anharmonic modes.

III. Franck−Condon Analysis

A. Calculational Details. In the Franck−Condon approximation the threshold ionization region is described by the overlap of the neutral wave function (typically the ground state) with wave functions of the cation and the relevant electronic energy differences between the neutral and cationic wave functions. Franck−Condon factors (FCFs) are the squares of these overlaps. Obtaining FCFs in full-dimensionality for C_3H (six degrees of freedom) is a considerable challenge and we do not do that here.

A separable, harmonic model is certainly feasible; however, this would be inadequate for some modes of this system, as discussed in the previous section. Specifically *c*-C_3H^+ is a first-order saddle point and also *l*-C_3H either is slightly bent or has a very flat bending potential. For these modes and the corresponding ones for *c*-C_3H and *l*-C_3H^+ we take a numerical approach to evaluate FCFs involving the highly nonharmonic modes. To do this, we identified the imaginary frequency modes of *c*-C_3H^+ and *l*-C_3H (linear) and then were able to identify very similar normal modes of *c*-C_3H and *l*-C_3H^+, respectively. We then obtained numerical potentials for these modes, corresponding numerical wave functions and finally numerical FCFs as described next.

First, consider the analysis for *c*-$C_3H \rightarrow$ *c*-C_3H^+. As noted, *c*-C_3H exists in a true minimum, whereas *c*-C_3H^+ is a saddle point. The imaginary frequency (mass-scaled) normal mode of *c*-C_3H^+ is shown in Figure 2 along with the normal mode of *c*-C_3H which most resembles the imaginary frequency one. These modes were obtained from the PESs and the mode of *c*-C_3H shown is labeled mode 2 in Table 2. Numerical FCFs for these two modes are then the ones of interest and we obtain them by assuming the normal modes are the same (obviously they are close but not identical) and so we ignore the "Duschinsky rotation" between them. We also ignore small differences in the reference geometries of *c*-C_3H and *c*-C_3H^+. Examination of the structures given Table 1 indicates that this too should be a good approximation. Thus, a direct calculation of the FCFs for these two modes assuming the normal modes are equal is a reasonable approximation.

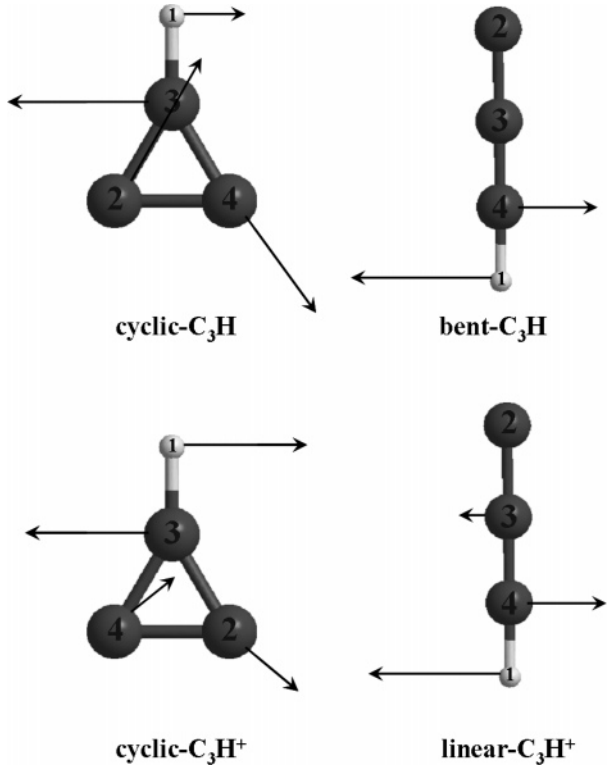

Figure 2. Imaginary-frequency normal mode of *c*-C_3H^+, corresponding real-frequency normal mode for *c*-C_3H, imaginary-frequency normal mode of *l*-C_3H, and corresponding real-frequency normal mode for *l*-C_3H^+.

Similar considerations for *l*-C_3H also lead to the conclusion that FCFs involving the imaginary frequency bending mode of *l*-C_3H in the linear geometry and an analogous bending mode in *l*-C_3H^+ should be a physically reasonable model. The relevant normal modes of the neutral and cation are also shown in Figure 2. The cation normal mode is the doubly degenerate bend with $\omega = 808$ cm^{-1}, and as seen, it is quite similar to the (doubly degenerate) imaginary frequency mode of *l*-C_3H (linear).

Having identified the imaginary frequency modes for *c*-C_3H^+ and *l*-C_3H and the similar real frequency ones for *c*-C_3H and *l*-C_3H^+ it remains to determine the corresponding potentials along these modes, all denoted generically as "Q", using the PESs and to solve the 1d Schrödinger equations for the eigenfunctions and eigenvalues. For the imaginary-frequency mode of *c*-C_3H^+ the full-dimensional PES was minimized with respect to the other normal modes as Q was varied starting at $Q = 0$, the saddle point. The same procedure was followed for one of the two degenerate imaginary-frequency modes of *l*-C_3H (linear). The resulting potentials are shown in Figures 3 and 4, respectively, where we also show the relaxed potentials along the corresponding real-frequency normal mode of *c*-C_3H and *l*-C_3H^+ in the respective figures. Note the potentials for the neutrals are zero at the local minima and the potentials for the corresponding cations include the electronic energy of the cation, measured relative to the zero potential value shown in these figures.

As seen in Figure 4, the relaxed *c*-C_3H^+ potential decreases from the saddle point value, where $Q = 0$, by 5700 cm^{-1} at the minimum, $Q = \pm 265$, which corresponds to the *l*-C_3H^+ structure, as it should. (From Table 2 the precise energy

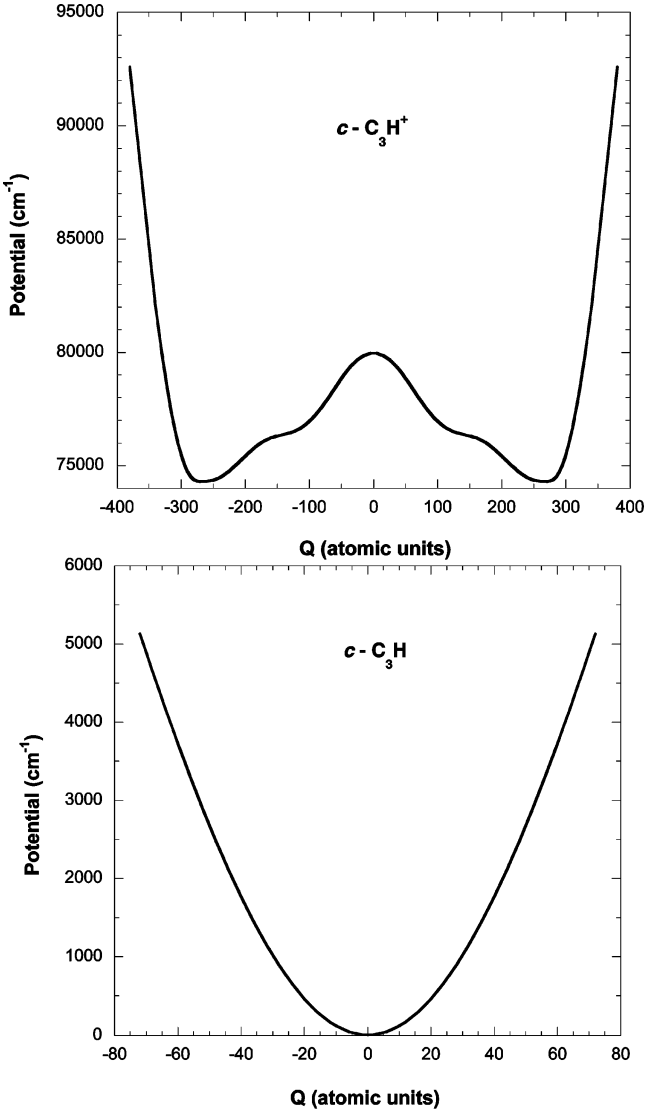

Figure 3. Relaxed potential for the imaginary frequency mode of c-C_3H^+ (top) and corresponding potential for the real frequency mode for c-C_3H (bottom). See text for more details.

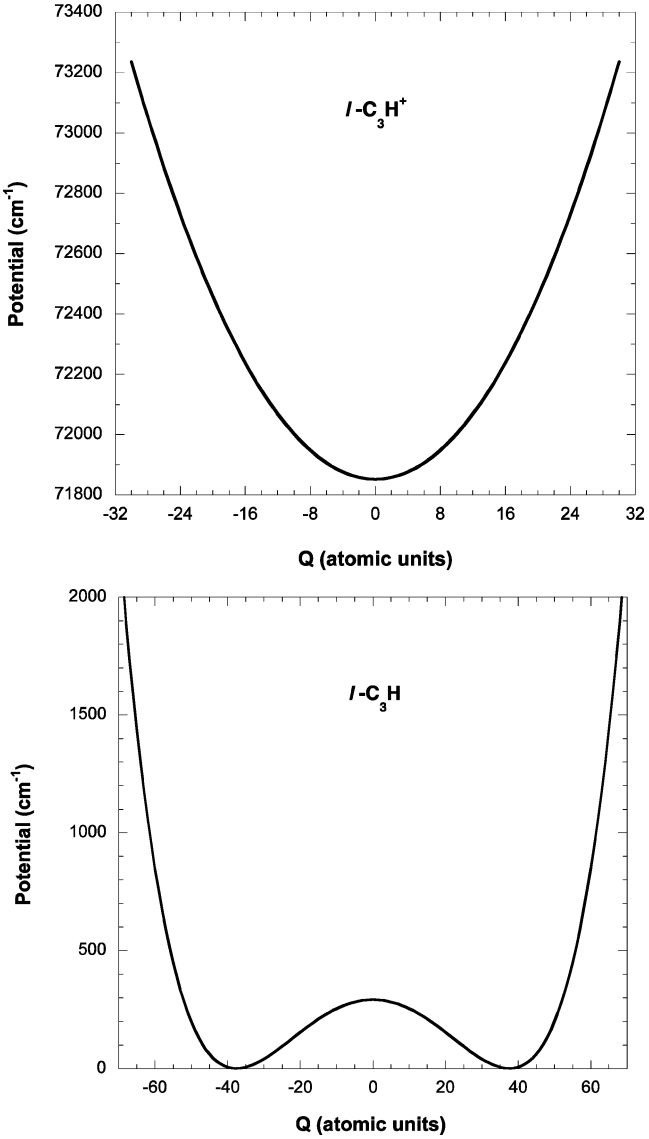

Figure 4. Relaxed potential for the real frequency mode of l-C_3H^+ (top) corresponding potential for the imaginary frequency mode for l-C_3H (bottom). See text for more details.

difference is 5667 cm^{-1}.) Beyond this value of Q the potential rises steeply, resulting in a double-well potential over the range of Q shown. If Q were an angular variable, the potential would be periodic as the system would return to another c-C_3H^+ configuration. This does not occur with the rectilinear normal mode and so the potential shown is valid for the region of Q shown and wave functions obtained with this potential are realistic for energies not very far in excess of the barrier energy. (As we will see later, this is sufficient for our analysis.)

The relaxed potential for the imaginary-frequency mode of l-C_3H is shown in Figure 4. As seen, this is a double well potential, as expected, with a barrier height of 300 cm^{-1}. The corresponding potential for l-C_3H^+ along the bending normal mode that is close in character to the imaginary frequency one of l-C_3H is also shown in this figure. As seen, it is, to a good approximation, quite harmonic.

The Schrödinger equation was solved for these four potentials numerically, using the equally spaced "Discrete Variable Representation" of the Cartesian kinetic energy operator due to Colbert and Miller.[30] Franck−Condon factors were then calculated numerically from these wave functions but restricted to the ground state wave functions for the neutrals, c-C_3H and l-C_3H.

B. Results and Discussion. The ground state wave function for the imaginary-frequency mode of l-C_3H, with potential given in Figure 4, is shown in Figure 5. The energy of this wave function, 215 cm^{-1}, is slightly below the barrier height of 300 cm^{-1}. As a result, the function has a small dip at $Q = 0$ and two peaks at approximately $Q = \pm 40$, where the numerical potential has identical minima. However, as seen, the wave function has considerable amplitude at $Q = 0$ and thus can be accurately characterized as being delocalized over the two minima and saddle point. This delocalization essentially removes the concern over whether the l-C_3H has its minimum at the linear geometry or a slightly bent one.

The ground state wave function for c-C_3H is shown in Figure 6 along with the excited state wave function of c-C_3H^+ that has the maximum overlap with it, and hence the largest FCF. The energy of this excited state wave function is 5700 cm^{-1}, relative to the minimum of the potential for the cation, plotted in Figure 4. This energy is nearly identical to the barrier height shown in that figure and, as expected, the wave function is concentrated in the region of the barrier, and thus has a substantial overlap with the ground state wave function of c-C_3H.

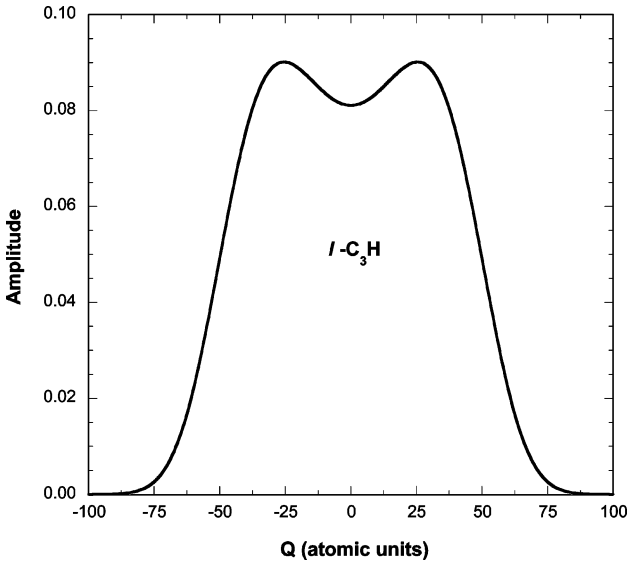

Figure 5. Ground state vibrational wavefunction for the relaxed potential of the imaginary frequency mode of *l*-C_3H shown in Figure 4.

The results of the Franck−Condon calculations are given in Figure 7, where FCFs are plotted versus energy. These FCFs are only for the 1d wave functions obtained from the four numerical potentials presented above. FCFs for all other modes were not calculated under the assumption that the largest FCF would be for the ground state to ground state transitions for these modes. This follows primarily from the similarity of the relevant neutral and cation equilibrium geometries.

Before discussing the FCFs, we explain how the energy axis was determined. Basically, these energies are differences in the full-dimensional ZPE for the two neutral species and the cations for which FCFs were calculated plus an appropriate electronic energy difference. The electronic energy differences were obtained from CCSD(T)/aug-cc-pVTZ calculations at the relevant PES geometries described below instead of the MP2 energy differences from the two PESs because the former energies are more accurate than the latter ones. For *l*-C_3H the full dimensional ZPE was obtained as the sum of the harmonic ZPE of all real-frequency modes of *l*-C_3H plus the ZPE obtained numerically for the doubly degenerate imaginary-frequency mode. The ZPE of *c*-C_3H was obtained similarly as the sum of the ZPE of the wave function shown in Figure 7 plus the harmonic ZPEs and for all other c-C_3H modes. For *l*-C_3H^+ the vibrational energies are the sum of the harmonic ZPEs for all real-frequency modes plus the numerically determined vibrational energies of wave functions determined from the potential shown in Figure 4. Relative to this origin, the cation energy for the *l*-C_3H FCFs was obtained using the accurate CCSD(T)/aug-cc-pVTZ energy difference between the equilibrium structures of *l*-C_3H (slightly bent) and *l*-C_3H^+ (linear) plus the vibrational energies of *l*-C_3H^+ obtained relative to the equilibrium structure of *l*-C_3H^+. The same procedure was followed for the energies of the FCFs for *c*-C_3H^+ with the origin of the 1d vibrational energies being the *l*-C_3H^+ equilibrium. The real-frequency modes of *c*-C_3H^+ are the ones at the saddle point geometry. The relevant electronic energy difference is the electronic energy of the equilibrium structure of *c*-C_3H and the electronic energy of *l*-C_3H^+ equilibrium, again obtained using CCSD(T)/aug-cc-pVTZ energies instead of the PES values.

Returning now to Figure 7 and considering first the FCFs for *l*-$C_3H \rightarrow$ *l*-C_3H^+ we see, as expected, a "textbook"

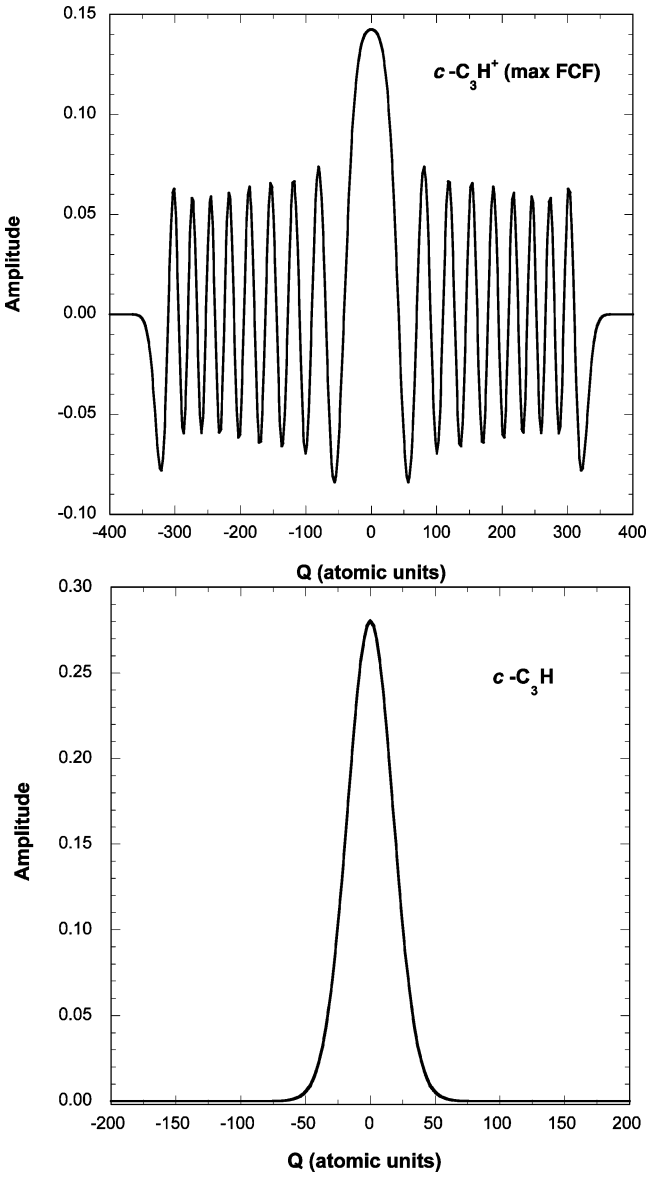

Figure 6. Ground state vibrational wave function for the relaxed potential of the real frequency mode of *c*-C_3H shown in Figure 3 (top) and the excited state vibrational wave function of *c*-C_3H^+ from the potential shown in Figure 3 (bottom) with the maximum overlap with the ground state wave function of *c*-C_3H shown.

progression with the largest FCF corresponding to the adiabatic transition, i.e., to the ground vibrational state of *l*-C_3H^+. The energy of this transition is 9.06 eV, and this represents the present vaule of the threshold energy for *l*-C_3H ionization. This value is 0.11 eV above the vertical ionization energy, without ZPE correction, of 8.95 eV given in the previous section.

Consider now the FCFs for *c*-$C_3H \rightarrow C_3H^+$. As seen, the maximum FCF occurs at 9.76 eV (the cation wave function corresponding to the FCF was shown in Figure 6), which is quite close to the vertical energy estimate to the saddle point of 9.8 eV given in the previous section. However, there are significant FCFs at lower energies, making the assignment of a threshold energy somewhat problematic. With this in mind a threshold ionization of *c*-C_3H in the range 9.70−9.76 eV is reasonable.

The present calculations of the threshold IPs will hopefully be of use in experimental determinations of them. A partial validation of the calculations does exist from a recent experi-

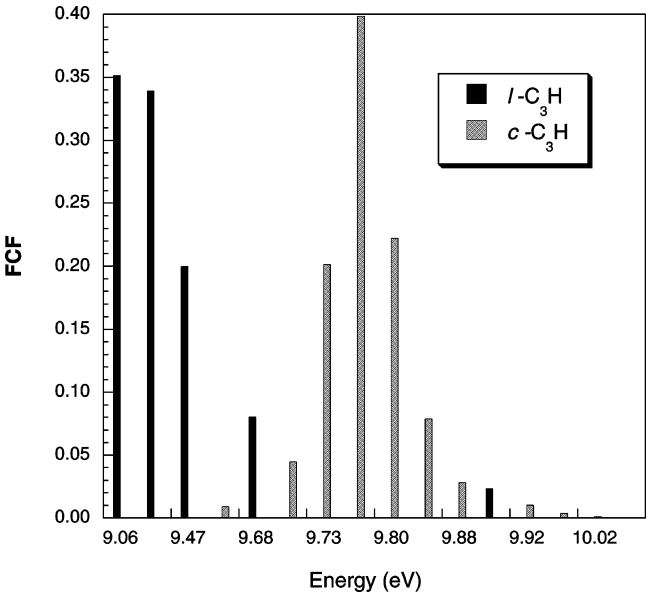

Figure 7. Franck−Condon factors for *l*-C_3H and c-C_3H ionization vs energy. See the text for a discussion of the energy axis.

ment, which reported a threshold IP of 9.7 ± 0.2 eV,[31,32] however, without resolving which isomer or isomers the measurement corresponds. The present calculations point to the *c*-C_3H isomer.

IV. Summary and Conclusions

We presented a Franck−Condon analysis in reduced dimensionality for the ionization thresholds of *l*-C_3H and *c*-C_3H using MP2-based potential energy surfaces and CCSD(T)/aug-cc-pVTZ calculations of electronic energies at selected geometries. Comparisons were made with previous electronic structure calculations for stationary point geometries and energies of the neutrals and cations.

Relaxed numerical potentials were determined along the imaginary frequency mode of *c*-C_3H^+, which exists as a first-order saddle point, and also along the imaginary frequency mode of *l*-C_3H, which on our PES also exhibits a saddle point structure at the strictly linear geometry. Corresponding, similar normal modes were identified for the *c*-C_3H and *l*-C_3H^+, and numerical potentials were also determined along these modes. Numerical solutions to the 1d Schrödinger were obtained and used to calculate the 1d Franck−Condon factors describing the ionization of *l*-C_3H and *c*-C_3H. From these results we reported ionization thresholds of 9.06 and 9.70−9.76 eV, respectively. These results differ from previous estimates in the literature, especially for *c*-C_3H, which did not consider a Franck−Condon analysis. Given the approximations made in this analysis we estimate that the present ionization energies are accurate to within roughly ±0.05 eV.

Acknowledgment. J.M.B. thanks the Department of Energy (DOE-DE-FG02-97ER14782) and B.B. thanks the Office of Naval Research (N00014-05-1-0460) for financial support. We thank one reviewer for pointing out references 31 and 32.

References and Notes

(1) Clary, D. C.; Buonomo, E.; Sims, I. R.; Smith, W. M.; Geppert, W. D.; Naulin, C.; Costes, M.; Cartechini, L.; Casavecchia, P. *J. Phys. Chem. A* **2002**, *106*, 5541.
(2) Smith, I. W. M. *Chem. Soc. Rev.* **2003**, *31*, 137.
(3) Kaiser, R. I.; Le, T. N.; Nguyen, T. L.; Mebel, A. M.; Balucani, N.; Lee, Y. T.; Stahl, T.; Schleyer, P. V. R.; Schaefer, H. F., III. *Faraday Discuss.* **2001**, *119*, 51.
(4) Clary, D. C.; Haider, N.; Husain, D.; Kabir, M. *Astrophys. J.* **1994**, *422*, 416.
(5) Turner, B. E.; Herbst, E.; Terzieva, R. *Astrophys. J. Suppl. Ser.* **2000**, *126*, 427.
(6) Keene, J.; Young, K.; Phillips, T. G.; Buttegenbach, T. H. *Astrophys. J.* **1993**, *415*, L131.
(7) Kaiser, R. I.; Ochsenfeld, C.; Head-Gordon, M.; Lee, Y. T.; Suits, A. G. *J. Chem. Phys.* **1997**, *106*, 1729.
(8) Haider, N.; Husain, D. *J. Chem. Soc., Faraday Trans.* **1993**, *89*, 7.
(9) Chastaing, D.; James, P. L.; Sims, I. R.; Smith, I. W. M. *Phys. Chem. Chem. Phys.* **1999**, *1*, 2247.
(10) Chastaing, D.; Le, Picard, S. D.; Sims, I. R.; Smith, I. W. M. *Astron. Astrophys.* **2001**, *365*, 241.
(11) Kaiser, R. I.; Stranges, D.; Lee, Y. T.; Suits, A. G. *Astrophys. J.* **1997**, *477*, 982.
(12) Kaiser, R. I.; Mebel, A. M.; Lee, Y. T. *J. Chem. Phys.* **2001**, *114*, 231.
(13) Cartechini, L.; Bergeat, A.; Capozza, G.; Casavecchia, P.; Volpi, G. G.; Geppert, W. D.; Naulin, C.; Costes, M. *J. Chem. Phys.* **2002**, *116*, 5603.
(14) Costes, M.; Daugey, N.; Naulin, C.; Bergeat, A.; Leonori, F.; Segoloni, E.; Petrucci, R.; Balucani, N.; Casavecchia, P. *Faraday Discuss. Chem. Soc.* **2006**, *133*.
(15) Ochsenfeld, C.; Kaiser, R. I.; Lee, Y. T.; Suits, A. G.; Head-Gordon, M. *J. Chem. Phys.* **1997**, *106*, 4141.
(16) Takahashi, J.; Yashimata, K. *J. Chem. Phys.* **1996**, *104*, 6613.
(17) Guadagnini, R.; Schatz, G. C.; Walch, S. P. *J. Phys. Chem. A* **1998**, *102*, 5857.
(18) Mebel, A. M.; Jackson, W. M.; Chang, A. H. H.; Lin, S. H. *J. Am. Chem. Soc.* **1998**, *120*, 5751.
(19) Buonomo, E.; Clary, D. C. *J. Phys. Chem. A* **2001**, *105*, 2694.
(20) Takayanagi, T. *Chem. Phys.* **2005**, *312*, 61.
(21) Takayanagi, T. *J. Phys. Chem. A* **2006**, *110*, 361.
(22) Park, W. K.; Park, J.; Park, S. C.; Braams, B. J.; Chen, C.; Bowman, J. M. *J. Chem. Phys.* **2006**, *125*, 081101.
(23) See for example, Cool, T. A.; Nakajima, K.; Mostefaoui, T. A.; Qi, F.; McIlroy, A.; Westmoreland, P. R.; Law, M. E.; Poisson, L.; Peterka, D. S.; Ahmed, M. *J. Chem. Phys.* **2003**, *119*, 8356.
(24) Ikuta, S. *J. Chem. Phys.* **1997**, *106*, 4536.
(25) Chaudhuria, R. K.; Majumder, S.; Freed, K. F. *J. Chem. Phys.* **2000**, *112*, 9301.
(26) Werner, H.-J.; Knowles, P. J.; Lindh, R.; Manby, F. R.; Schutz, M.; Celani, P.; Korona, T.; Rauhut, G.; Amos, R. D.; Bernhardsson, A.; Berning, A.; et al. MOLPRO, 2006.1 ed., 2006.
(27) Xie, Z.; Braams, B. J.; Bowman, J. M. *J. Chem. Phys.* **2005**, *122*, 224307.
(28) Sharma, A. R.; Wu, J.; Braams, B. J.; Carter, S.; Schneider, R.; Bowman, J. M. *J. Chem. Phys.* **2006**, *125*, 224306.
(29) Stanton, J. *Chem. Phys. Lett.* **1995**, *237*.
(30) Colbert, D.; Miller, W. H. *J. Chem. Phys.* **1982**, *96*, 992.
(31) Benedikt, J.; Eijkman, D. J.; Vandamme, W.; Agarwal, S.; Van de Sanden, M. C. M. *Chem. Phys. Lett.* **2005**, *402*, 37.
(32) Benedikt, J.; Agarwal, S.; Eijkman, D.; Vandamme, W.; Creatore, Mariadriana; van de Sanden, M. C. M. *J. Vac. Sci. Technol. A* **2005**, *23*, 1400.